Levels of ^{53}Mn with the ^{52}Cr(^{3}He, d)^{53}Mn and ^{52}Cr(^{7}Li, ^{6}He)^{53}Mn reactions*

G. D. Gunn,† J. D. Fox, and G. J. KeKelis‡
Department of Physics, The Florida State University, Tallahassee, Florida 32306
(Received 16 December 1974)

The levels of ^{53}Mn populated by the reactions ^{52}Cr(^{3}He, d)^{53}Mn at 24 MeV and ^{52}Cr(^{7}Li, ^{6}He)-^{53}Mn at 34 MeV were studied using The Florida State University quadrupole spectrometer. Angular distributions were taken from 5° to 60° for ^{52}Cr(^{3}He, d)^{53}Mn, and from 1° to 25° for the ^{52}Cr(^{7}Li, ^{6}He)^{53}Mn reaction. Angular distributions show the expected L-dependent shapes which are well described by the distorted wave Born approximation. Relative spectroscopic factors are in excellent agreement with previous studies. The J-dependent shape of the (^{7}Li, ^{6}He) angular distributions at forward angles is used to identify the 2.68 and 3.48 MeV levels as $p_{1/2}$, and the 4.07 and 4.43 MeV levels as $p_{3/2}$. Absolute spectroscopic factors for the two reactions are in very good agreement and are about 30% lower than the values of previous studies. Seventeen levels of ^{53}Mn above 6 MeV are observed in one or both reactions. Angular distributions for eight levels are extracted for the (^{3}He, d) reaction, including the three isobaric analog levels at 6.97, 7.54, and 8.03 MeV. Several of the levels above 6 MeV exhibit angular distributions which might be interpreted as being for either $l=3$ or $l=4$ transferred. These levels are identified as g-wave final states on the basis of their strength and excitation energy. The spectroscopic factors for the unbound levels are derived by a technique of extrapolation of cross sections from the bound state analysis. The spectroscopic factors extracted for the isobaric analog levels are consistent with (d, p) results to the parent states, within the limitations of the analysis.

[NUCLEAR REACTIONS ^{52}Cr(^{3}He, d)^{53}Mn, $E=24$ MeV; ^{52}Cr(^{7}Li, ^{6}He)^{53}Mn, $E=34$ MeV; measured $\sigma(\theta)$; DWBA analysis; ^{53}Mn levels; deduced J^{π} and spectroscopic factors; enriched targets.]

I. INTRODUCTION

Direct single nucleon transfer reactions have been used to extract spectroscopic information about nuclei for many years. The use of the distorted wave born approximation (DWBA) in the analysis of direct reactions has been successful in the extraction of transferred orbital angular momenta and spectroscopic factors. The light ion (d, n), (^{3}He, d), and (α, t) reactions have often been used to study proton particle configurations. Recently, heavy ion stripping reactions, such as the (^{16}O, ^{15}N) and (^{14}N, ^{13}C) reactions, have come under study. These reactions present the opportunity to study the transfer reaction when the nucleon to be transferred is not in a predominantly s state in the projectile. An important experimental drawback to these heavy ion reactions is the poor energy resolution generally obtained. The (^{7}Li, ^{6}He) reaction allows one to study the transfer of a proton from a relative p-wave orbit in the projectile, but does not suffer so extremely from the problem of resolution.

The levels of ^{53}Mn have been studied with all three light ion proton stripping reactions mentioned above,[1-7] and many of these results are tabulated in Table I, and can be found in the Nuclear Data sheets.[8] Additionally, a study using the (^{12}C, ^{11}B) and (^{14}N, ^{13}C) reactions has been reported,[9-10] although the systematics of the reaction mechanism was the intent of that study.

The Florida State University quadrupole spectrometer has been used to study the ^{52}Cr(^{3}He, d)^{53}Mn reaction and the ^{52}Cr(^{7}Li, ^{6}He)^{53}Mn reaction. In the (^{3}He, d) study, a number of levels up to 8 MeV excitation are identified and l values and spectroscopic factors were extracted from the angular distributions through the use of zero range DWBA analysis. Some new levels above 6 MeV are reported, and g-state strength is tentatively identified. Angular distributions of the isobaric analogs of the first three levels of ^{53}Cr were measured. In the (^{7}Li, ^{6}He) reaction, forward angle data were taken in to 1° (lab) and the J dependence of the reaction was used to extract final state J values for several levels. Spectroscopic factors were extracted using exact finite range DWBA analysis.

II. EXPERIMENTAL PROCEDURE

The ^{3}He^{-} beam was produced in a duoplasmatron source using a closed ^{3}He recovery system to reduce gas consumption. Negative ion beams of ^{7}Li were produced in a Heinicke radial extraction source.[11] The Florida State University Super FN tandem Van de Graaff accelerator was used to accelerate the ^{3}He beam to an energy of 24 MeV and the ^{7}Li beams to 34 MeV. Typical beam intensi-

TABLE I. Spectroscopic information for levels of ^{53}Mn populated through proton stripping reactions. Brackets [ ] indicate FRDWBA calculations used for (^{3}He,d). Parentheses ( ) in C^2S column for previous work indicates $(2J+1)C^2S$ is quoted.

	Excitation energy							Spectroscopic factor (C^2S)					
	Present work							Present work					
	(^{3}He,d)	(^{7}Li,^{6}He)	(^{3}He,d) [a]	(^{3}He,d) [b]	(^{3}He,d) [c]	(d,n) [d]	l_j	(^{3}He,d)	(^{7}Li,^{6}He)	(^{3}He,d) [a]	(^{3}He,d) [b]	(^{3}He,d) [c]	(d,n) [d]
1	0.00	0.00	0.00	0.00	0.00	0.0	$f_{7/2}$	0.23 [0.22]	0.41	0.47	0.51	0.42	0.42
			0.38	0.385	0.383	···	$_{5/2}$	···	···	···	···	···	···
2	1.29	1.29	1.29	1.296	1.296	1.29	$p_{3/2}$	0.04	0.05	0.07	0.06	0.04	0.05
	(2.37)			2.370		···	p	···	···	···	(0.04)	···	···
3	2.41	2.41	2.40	2.413	2.410	2.36	$p_{3/2}$	0.28 [0.26]	0.32	0.45	0.43	0.43	0.28
4	2.68	2.68	2.66	2.678	2.677	2.60	$p_{1/2}$	0.15 [0.14]	0.14	0.22	0.16	0.21	0.25
				2.720	2.720	···	$(s_{1/2})$	···	···	···	(0.05)	(0.02)	···
5	2.88	2.88	2.88	2.882	2.886	2.90	$p_{3/2}$	0.03	0.01	0.02	0.02	0.03	0.02
				3.010		···	(d,f)	···	···	···	(0.05, 0.08)	···	···
		3.06	3.10	3.061	3.065	···	$f_{5/2}$	···	0.03	0.04	0.02	0.01	···
6	3.10		3.10	3.104	3.114	···	$p_{3/2}$	0.02	···	0.02	0.02	0.02	···
7	3.48	3.48	3.47	3.484	3.496	3.42	$p_{1/2}$	0.10	0.15	0.17	0.15	0.15	0.16
8	3.67	3.67	3.67	3.669	3.679	···	$f_{5/2}$	0.21 [0.21]	0.27	0.39	0.22	0.44	···
9	3.90	3.90	3.90	3.900	3.897	3.93	$p_{3/2}$	0.01	···	0.02	0.02	0.04	0.04
					3.977	···	$(s_{1/2})$	···	···	···	···	(0.05)	···
10	4.07 [e]	4.07 [e]	4.07 [e]	4.070 [e]	4.075	···	$p_{(3/2)}$	0.01	0.02	0.02	0.02	0.03	···
	4.07 [e]	4.07 [e]	4.07 [e]	4.070 [e]		···	$f_{5/2}$	0.07	0.11	0.17	0.07	···	···
					4.214	···	p	···	···	···	···	(0.01)	···
11	4.29	4.30	4.29	4.278	4.290	···	$f_{5/2}$	0.02	···	0.07	0.15	0.06	···
				4.304		···	f	···	···	···	(0.16)	···	···
	(4.35)			4.358	4.346	···	$p(s_{1/2})$ [f]	···	···	···	(0.04) [f]	(0.09) [f]	···
12	4.43	4.44	4.43	4.434	4.446	4.35	$p_{(3/2)}$	0.06	0.04	0.07	0.06	0.09	0.07
13	4.57 [e]	4.57	4.57 [e]	4.569	4.583	···	$p_{(1/2)}$	0.02	···	0.05	0.05	0.08	···
	4.57 [e]		4.57 [e]			···	$f_{(5/2)}$	0.03	···	0.04	···	···	···
14	4.72	4.72	4.74	4.721	4.737	4.71	$p_{(1/2)}$	0.13	···	0.20	0.14	0.24	0.27
	(4.78)			4.788	4.800	···	$(p)(s_{1/2})$ [f]	···	···	···	(0.03) [f]	(0.06) [f]	···
15	4.96 [e]	4.96	4.96	4.936		···	$f_{(5/2)}$	0.11	···	0.15	0.05	···	···
	4.96 [e]		4.96	4.957	4.967	4.95	$p_{(1/2)}$	0.04	···	0.07	0.09	0.17	0.07
16	5.08	5.08	5.08	5.085	5.105	5.12	$p_{(1/2)}$	0.06	···	0.08	0.06	0.12	0.11
17	5.32			5.322	5.310		$p_{(1/2)}$	0.03				[g]	
18	5.49	5.48		5.485			$p_{(1/2)}$	0.02			0.03	···	
19	5.58			5.586									
20	5.68			5.705									
21	5.79			5.800									
22	5.89	5.86		5.886									
	(5.95)												

TABLE I *(Continued)*

	Excitation energy							Spectroscopic factor (C^2S)					
	Present work							Present work					
	(^{3}He,d)	(^{7}Li,^{6}He)	(^{3}He,d) [a]	(^{3}He,d) [b]	(^{3}He,d) [c]	(d,n) [d]	l_j	(^{3}He,d)	(^{7}Li,^{6}He)	(^{3}He,d) [a]	(^{3}He,d) [b]	(^{3}He,d) [c]	(d,n) [d]
23	6.01	6.01		6.005									
24	6.15	(6.15)											
25	6.24	(6.23)											
26	6.32	(6.32)											
27	6.41	(6.43)											
28	6.49												
29	6.54	6.53					$(g_{9/2})$	0.31					
30	6.73												
31	6.87												
32	6.97	6.95					$p_{3/2}$	0.20					
33	7.10	7.09					$(g_{9/2})$	0.10					
34	7.25	7.22					$g_{9/2}$	0.07					
35	7.36						$f_{(5/2)}$	0.11					
36	7.45												
37	7.54	7.54					$p_{1/2}$	0.18					
38	7.78	7.77					$f_{(5/2)}$	0.03					
39	7.91						$g_{9/2}$	0.03					
40	8.03	8.01					$f_{5/2}$	0.11					

[a] Reference 5.
[b] Reference 6, not corrected for spin orbit.
[c] Reference 7.
[d] Reference 1.
[e] Unresolved doublets.
[f] Disagreement between Ref. 4 and 5 as to l.
[g] Identified by Ref. 7 as s-wave state.

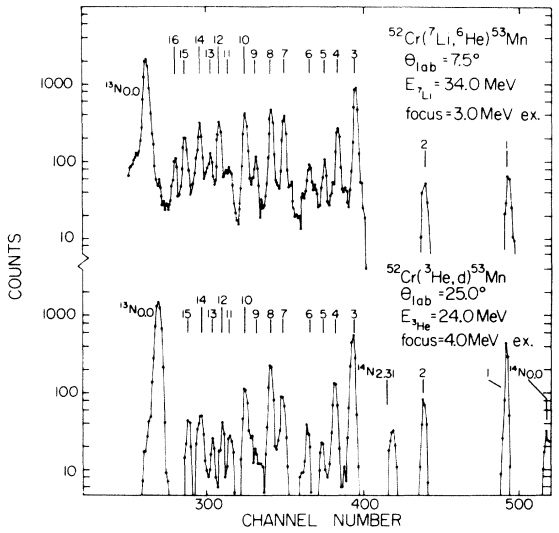

FIG. 1. Spectra from the ^{52}Cr(^{3}He,d)^{53}Mn reaction and the ^{52}Cr(^{7}Li,^{6}He)^{53}Mn reaction. Numbering of the peaks corresponds to the numbering in Table I. Each of these spectra is at the stripping peak for p-wave final states, and the similar relative intensities for the two reactions going to the various levels is evident.

ties on target were 200 nA and 150 nA for the ^{3}He and ^{7}Li beams, respectively. The targets for the early runs to investigate levels with excitation energies of less than 5 MeV were of Cr_2O_3 enriched to 98% ^{52}Cr, evaporated on thin natural carbon backings. These targets were used for all studies on the ^{52}Cr(^{7}Li,^{6}He)^{53}Mn reaction. For later runs using the ^{52}Cr(^{3}He,d)^{53}Mn reaction to study the higher excitation energy levels of ^{53}Mn, self-supporting targets were made by evaporation of metallic chromium onto a copper backing; the copper was then etched off with hydrochloric acid. The evaporated targets were 50 μg/cm^2, and the self-supporting targets were 200 μg/cm^2 in thickness. The self-supporting targets were found to be too thick for use in the ^{52}Cr(^{7}Li,^{6}He)^{53}Mn reaction.

Angular distributions were taken in the Florida State University quadrupole spectrometer[12] (QDS) using a counter telescope placed at the focus in the detector chamber. High lying levels in both reactions were studied with the quadrupole lenses set to focus particles with magnetic rigidities corresponding to deuterons or ^{6}He's leaving ^{53}Mn at 7 MeV excitation. To study the lower levels, a 4 MeV focus was set for the (^{3}He, d) reaction and a 3 MeV focus was set for the (^{7}Li, ^{6}He) reaction. The angular distributions were taken from 5° to 40° in 5° increments for the 4 MeV focus in the (^{3}He, d) study, and from 5° to 25° in 2.5° steps and from 30° to 60° in 5° steps for the 7 MeV focus.

For the ^{52}Cr(^{7}Li, ^{6}He)^{53}Mn reaction, angular distributions were taken from 5° to 25° in increments of 2.5°, and at 1° and 3° when possible.

For the (^{3}He, d) reaction, a 380 μm or a 320 μm ΔE detector was used in conjunction with a 3 mm Si(Li) detector. In the (^{7}Li, ^{6}He) study, a 94 μm ΔE detector was used with a 690 μm E detector. Detectors were cooled to −30° for all runs. The two dimensional events were delivered to the on-line computer and sorted into one dimensional particle-identified energy spectra by setting digital gates in the computer. Typical energy spectra for the ^{52}Cr(^{3}He, d)^{53}Mn and for the ^{52}Cr (^{7}Li, ^{6}He)^{53}Mn reactions are shown in Fig. 1. The numbering of the peaks corresponds to the level energies given in Table I.

A monitor counter was used throughout the experiments to make angle to angle normalization corrections. Data were also taken at selected angles in a large multipurpose scattering chamber to make corrections for the band pass of the QDS. Typical resolution in the QDS was 50 keV full width at half-maximum (FWHM) and 70 keV FWHM for the (^{3}He, d) reaction on the evaporated and on the self-supporting targets, respectively. For the (^{7}Li, ^{6}He) reaction in QDS, 65–80 keV FWHM was obtained as typical values for the resolution. In the scattering chamber, 70 keV resolution was achieved for the (^{3}He, d) reaction on the evaporated target, and 100–130 keV FWHM resolutions were typical on this target for the (^{7}Li, ^{6}He) reaction.

Extraction of peak yields was a problem. The ^{13}C impurity in the carbon backing of the targets, obscured levels of ^{53}Mn, especially at more forward angles. Above 5 MeV excitation in ^{53}Mn, ^{13}N, and ^{17}F impurity peaks dominated the spectrum and made it impossible to find levels at some angles. The use of the self-supporting natural chromium targets lessened the carbon and oxygen impurity problem. The spectra at many angles were compared with those from the enriched targets to identify any impurities of other chromium isotopes. Another difficulty in reduction of the data was the high density of states above 6 MeV in excitation. Often the level density did not allow peaks to be completely resolved. At the low energy (high excitation energy) region of the spectra, the background did not increase exponentially due to the focusing properties of the spectrometer. Extraction of yields in this region was troublesome due to the difficulty in determining the shape of the background.

The band pass efficiency curve was determined by extracting the ratios of spectrometer data to data taken in a conventional scattering chamber at selected angles. To convert yields to cross sections, elastic scattering data were taken in the

scattering chamber at low energies. A target thickness-solid angle product was deduced from this data and folded into the scattering chamber to spectrometer (SC : QDS) ratio.

To obtain the energy calibration of the spectra, a quadratic least-squares fit was performed on the outgoing particle energies versus channels for the ground states of the ^{13}N and ^{17}F impurities, and for the ground state of ^{53}Mn, using the peaks from the entire angular range. The excitation energies of the levels were then calculated using the kinematic information. Excitation energies quoted in this paper are accurate to ±15 keV.

Errors in the absolute and relative cross sections were a function of the type of data involved. For the (^{3}He, d) reaction to levels up to 5.5 MeV in excitation, errors in the absolute cross sections were from 10% to 15%. Relative errors among the data points are 5% to 12%. For the (^{3}He, d) reaction to the levels above 5.5 MeV in excitation, errors in the absolute cross sections were from 15% to 25%. The relative error in this case was from 10% to 20%. For the (^{7}Li, ^{6}He) reaction, the absolute error is estimated to be 15% to 25% and the relative error is 12% to 20%.

The main source of the absolute errors was the uncertainty in the SC : QDS correction factor, which in turn was due to uncertainties in the scattering chamber yield and fitting uncertainty. Relative error is a result of the statistical errors and the fitting uncertainty. Other sources of error common to all of the cases above are the uncertainty in the angle setting in the scattering chamber and the uncertainty in the target thickness-solid angle product. Dead times were monitored and were generally less than 2%, except in the (^{7}Li, ^{6}He) runs at 1°, where the dead time ran to about 7%.

III. DATA ANALYSIS

A. General

The levels observed in the ^{52}Cr(^{3}He, d)^{53}Mn reaction at 24 MeV are given in Table I. Quoted excitation energies are accurate to ±15 KeV. Levels observed in the studies of Armstrong and Blair[5] (AB), O'Brien *et al.*[6] (ODBR), and Cujec and Szöghy[7] (CS) are also given. No new levels under 6 MeV are observed. The level at 0.38 MeV may have been weakly excited in this study, but statistics were never sufficient to identify this level. Several levels between 2.4 and 5 MeV were not observed due to insufficient resolution or statistics. The levels at 2.37, 2.72, and 4.35 MeV were sometimes observed as "shoulders" to larger peaks, but no angular distributions could be extracted. The levels between 5.75 and 6.55

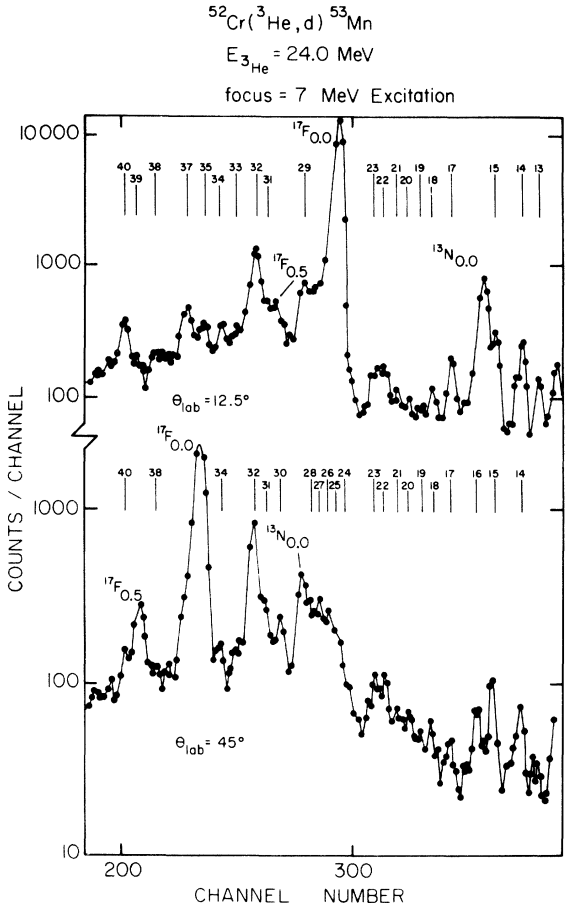

FIG. 2. Spectra of the ^{52}Cr(^{3}He,d)^{53}Mn reaction at 24 MeV and quadrupole lenses focused for deuterons leaving ^{53}Mn at 7 MeV excitation. Numbering of the peaks corresponds to the numbering in Table I.

MeV appear in the spectrum as two poorly resolved groups centered at 5.9 and 6.3 MeV. No angular distributions could be confidently extracted for any of these levels, excepting the level at 6.54 MeV, where the leading edge of the peak was used to establish the peak shape so that the yield could be extracted at many angles. Several other levels above 6.6 MeV were also not resolved sufficiently at enough angles to make it possible to extract a meaningful angular distribution from the data. The two spectra in Fig. 2 show the levels from 4.4 to 8.1 MeV and give some indication as to the difficulties involved in reducing the data for the higher lying levels. Numbering of the peaks corresponds to that in Table I. The spectra chosen are at 12.5° and 45° (lab) to show all of the identified levels.

The levels observed in the ^{52}Cr(^{7}Li, ^{6}He)^{53}Mn reaction at 34 MeV are also listed in Table I. Due to the poorer resolution and the impurity peaks,

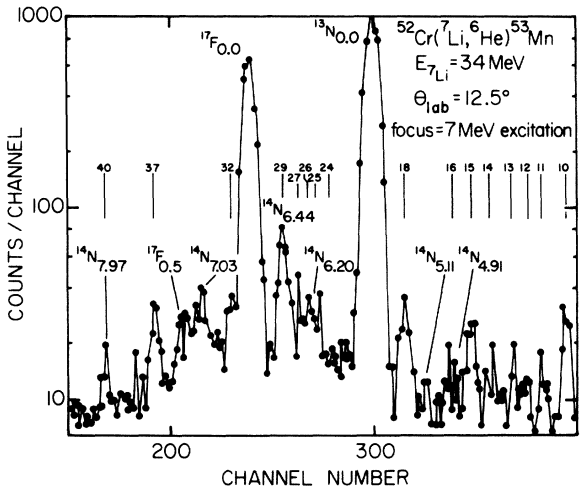

FIG. 3. Spectrum for the ^{52}Cr(^{7}Li, ^{6}He)^{53}Mn reaction at 34 MeV and 12.5° lab. The quadrupole lenses are focused for ^{6}He's leaving ^{53}Mn at 7 MeV excitation. Numbering of the peaks corresponds to the numbering in Table I.

fewer levels were identified in this reaction. Additionally, for the p-wave levels especially, the cross sections were much smaller, and fewer angular distributions were extracted. Figure 3 is a spectrum for the ^{52}Cr(^{7}Li, ^{6}He)^{53}Mn reaction at 12.5° (lab) showing the high-lying levels populated in this reaction. Even the levels at 6.54, 6.97, and 7.54 MeV, which have large cross sections in the (^{3}He, d) reaction, are not populated very strongly. Thus, the presence of impurity peaks coupled with the poorer resolution for this reaction and the reduced population of the levels makes it virtually impossible to extract usable angular distributions for any of the higher excited levels.

B. ^{52}Cr(^{3}He,d)^{53}Mn reaction data

Angular distributions of levels populated in the ^{52}Cr(^{3}He, d)^{53}Mn reaction at 24 MeV up to 5.49 MeV in excitation energy are displayed in Fig. 4. The p-wave final states show similar diffraction-like patterns with a forward angle peak at 8° (c.m.). The f-wave final states have less structured angular distributions, with the "stripping

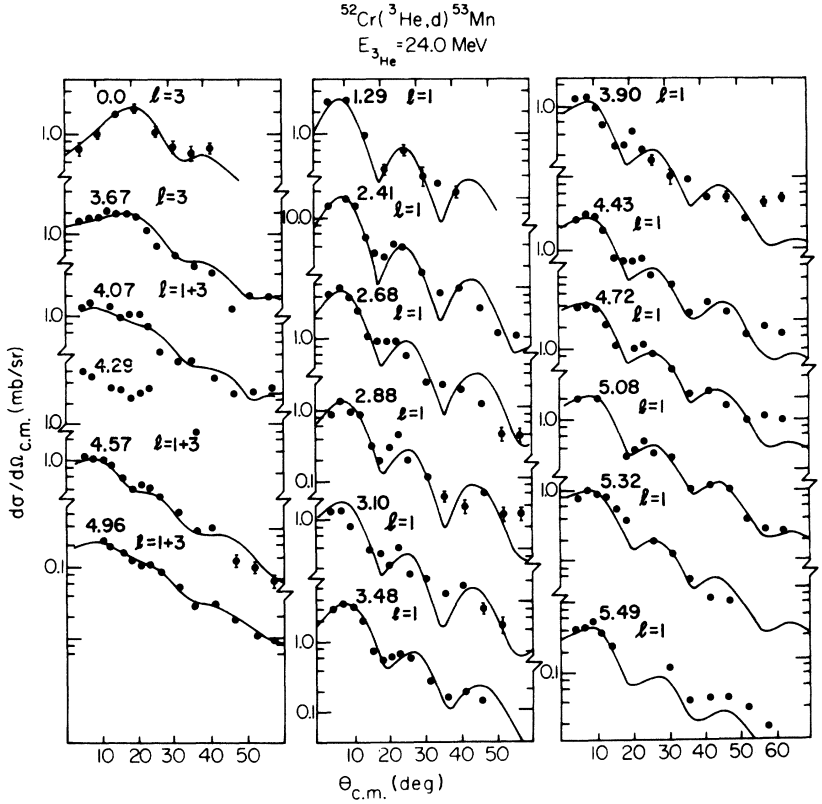

FIG. 4. Angular distributions for ^{52}Cr(^{3}He,d)^{53}Mn at 24 MeV up to 5.49 MeV excitation. Lines drawn are zero-range DWBA calculations.

TABLE II. Optical model parameters for the ^{52}Cr(^{3}He,d) ^{53}Mn reaction at 24 MeV. Parameters used as defined in Ref. 15.

Set	U (MeV)	r_R (fm)	a_R (fm)	W_S (MeV)	W_D (MeV)	r_I (fm)	a_I (fm)	r_C (fm)	λ
				^{3}He					
I [a]	98.8	1.069	0.814	13.5	···	1.705	0.726	1.069	
II [b]	167.2	1.07	0.804	16.92	···	1.73	0.597	1.4	
III [c]	165.0	1.43	0.613	30.3	···	1.50	0.710	1.4	
IV [c]	142.4	1.36	0.650	12.67	···	1.755	0.781	1.4	
				Deuterons					
I & III [d]	89.7	1.15	0.81	···	19.4	1.34	0.68	1.15	
II [b]	112.0	1.0	0.90	···	18.0	1.55	0.47	1.3	
^{52}Cr + p	Var.	1.25	0.65	···				1.25	25
d + p		1.25	0.65					1.25	25

[a] Reference 5.
[b] Reference 6.
[c] Reference 12.
[d] Reference 13.

peak" occurring at 21° (c.m.). The levels at 4.07, 4.29, 4.57, and 4.96 MeV do not have angular distributions resembling either pure f-wave or p-wave shapes. These levels, except for the 4.29 MeV level, are expected to be unresolved doublets of different orbital angular momentum.[5] The error bars shown represent the statistical counting errors only. Error bars are not shown when the data point is larger than the error. DWBA analysis of the levels was performed with the zero range DWBA code DWUCK.[13] Several sets of optical model parameters were tested to see if they would reproduce the experimental results. These sets were taken from the literature, and are tabulated in Table II. ^{3}He optical model parameter sets I and II were taken from the work of AB and ODBR, respectively; the sets III and IV are from the ^{52}Cr(^{3}He, α)^{51}Cr study at 18 MeV of Stock *et al.*[14] All of these parameter sets were derived from fitting elastic ^{3}He scattering data at the appropriate energy. Deuteron optical model parameters for Set I are from the work of Perey and Perey,[15] and were used with ^{3}He Sets I, III, and IV. Deuteron Set II was taken from ODBR.

Calculations with sets I, II, and III for the $f_{7/2}$ ground state and the $p_{3/2}$ 2.41 MeV level are displayed in Fig. 5. As can be seen, all of these optical model parameter sets give essentially equivalent shape reproduction on the angular distributions, although Set I seems to do a slightly better job of reproducing the shape of the ground state angular distribution at forward angles. The calculated curves are all normalized by the factor 4.42 and by the spectroscopic factor of 0.47 for the ground state and 0.45 for the 2.41 MeV level. These spectroscopic factors are those of AB. A difference of up to 50% is apparent for the predicted magnitudes; however, this difference was not considered sufficient justification to choose any one of the sets over the others, as it involves making a choice based on the assumption that both

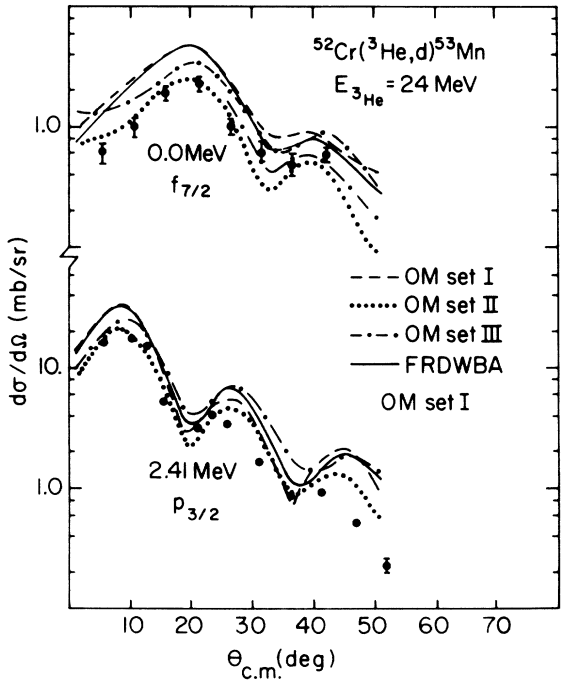

FIG. 5. Comparison of DWBA calculations using a variety of optical model parameter sets for the ^{52}Cr(^{3}He, d)^{53}Mn reaction at 24 MeV. Set numbers indicate both ^{3}He and d sets. The solid line is a FRDWBA calculation made with the code MERCURY using the parameters of Set I.

the zero-range factor of 4.42 and the spectroscopic factor used in this test are correct. On the basis of the better reproduction of the shape of the ground state angular distribution, the fact that the experimental beam energy 22 MeV was closer to that of this study, and the similarity among the calculations, optical model parameter Set I was used to make the calculations for comparison with the data. Use of a nonlocality correction factor of 0.77 raises the predicted DWBA cross section by 10%. AB used a radial cutoff of 4.2 fm in analyzing their data with this parameter set. For the p-wave level, no significant difference is visible over the angular range of 55°. For the f-wave level, the radial cutoff predicts a more rapid decrease of the cross section forward of 20° than the nonradial cutoff calculation. This rapid decrease was not reflected in the data and indicates that the radial cutoff scheme may in fact give a worse fit to the experimental results. No radial cutoff was used in making the DWBA calculations for comparison with the experimental results. Finite range (FR) calculations performed with the parameters of Set I using the code MERCURY[16] are also shown in Fig. 5. The bound state parameters used for the $d+p$ bound state were the same as those for the $^{52}Cr+p$ bound state, with the well depth adjusted to bind the proton to the deuteron with an energy of 5.49 MeV, the proton separation energy in ^3He. The spectroscopic factors of AB were again used to normalize the calculation, and 1.5 was used as the $d+p$ spectroscopic factor. The magnitude is in excellent agreement with that of the zero-range calculation, although some differences appear in the shapes of the angular distributions due to the use of the finite range (Woods-Saxon potential) form factor. The finite range calculation did not take into account the 7% D state of the ^3He.

The zero-range DWBA calculations made with the optical model parameter Set I are shown with the data in Fig. 4. The unresolved doublets at 4.07, 4.57, and 4.96 MeV have been fitted with DWBA calculations for $l=1$ and $l=3$ components. Spectroscopic factors derived from the comparison of the DWBA calculations with the data are given in Table I. The spectroscopic factor for the ground state is felt to have a large error since the band pass correction for this level was large. The spectroscopic factors found in the previous ($^3He, d$) studies are also given. The spectroscopic factors were calculated using the traditional normalization of 4.42,[17] which agrees to within 10% with the values calculated by Lim.[18] In their analysis, AB used a normalization constant of 3.7, found by analysis of the $^{48}Ca(^3He, d)^{49}Sc$ reaction, and additionally AB normalized the spectroscopic

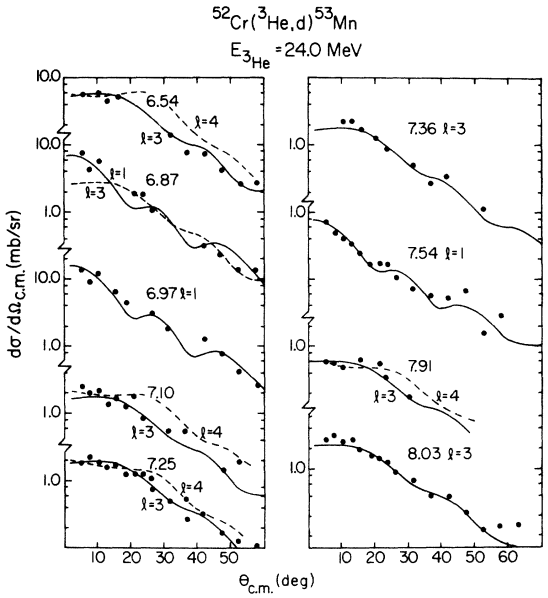

FIG. 6. Angular distributions for $^{52}Cr(^3He, d)^{53}Mn$ at 24 MeV for levels above 6.5 MeV. Lines drawn are zero-range DWBA calculations.

factors to bring the summed strength of the f-wave states into agreement with the total spectroscopic strength predicted from simple shell model calculations. This will be discussed further in Sec. V. ODBR used the value of 2.6 for the normalization on the basis of agreement of the strength of the $f_{7/2}$ state with the predicted strength. As can be seen, the values of C^2S found in this study are generally lower by 30% from the values found in the previous studies, although the relative spectroscopic factors from level to level are in very good agreement. The spectroscopic factors derived from the FRDWBA calculations for several selected levels are in excellent agreement with the present zero-range spectroscopic factors. These values are indicated by brackets in Table I.

Angular distributions for the levels from 6.54 to 8.03 MeV are shown in Fig. 6. All of these levels are unbound, with the exception of the 6.54-MeV level; the $^{52}Cr+p$ threshold is at 6.56 MeV. The levels at 6.97 and 7.54 MeV are identified as isobaric analog states (IAS) to the ground state and the 0.56 MeV first excited state of ^{53}Cr. These two levels are both p-wave states. The level at 6.87 MeV always appears in the spectra as a shoulder to the large 6.97 MeV level, and this made the extraction of the angular distribution somewhat difficult. As a result, the shape is not well enough defined to determine the orbital angular momentum transferred in populating this level. The level at 8.03 MeV is identified as the isobaric

analog state to the $f_{5/2}$ 1.01 MeV level in ^{53}Cr. The other angular distributions have shapes which may be interpreted as either f-wave or g-wave transfers, and the DWBA calculation is needed to establish the orbital angular momentum of the levels. DWBA calculations were performed and are shown in Fig. 6 with the experimental results. In order to make the calculations for the unbound levels, the form factors were calculated using a small binding energy of 0.1 MeV. Fortune *et al.*[19] have shown that this treatment is adequate in determining the shape of the unbound levels at forward angles. The bound state form factor was again integrated out to 16 fm in 0.1 fm steps. It was found that by integrating out to 20 and 25 fm, the forward angle cross section changed less than 5%, and the cross section for more backward angles changed less than 2%. The angular distributions of the IAS levels at 6.97 and 7.54 MeV are both well fitted by the p-wave calculations, and the angular distribution of the level at 7.36 MeV and the IAS at 8.03 MeV are well reproduced by f-wave calculations. The levels at 6.54, 7.10, 7.25, and 7.91 MeV are all identified as being g-wave levels, although for some of these levels the calculated f-wave angular distribution might be considered as an equally good fit to the data, as can be seen in Fig. 6. These assignments are made on the argument that should they be $l=3$ levels, there would be too much total f strength. Additionally, the cluster of levels from 6.2 to 6.54 MeV have a rather characteristic shape in the spectra which persists throughout the angular distribution, and although the other levels were not explicitly

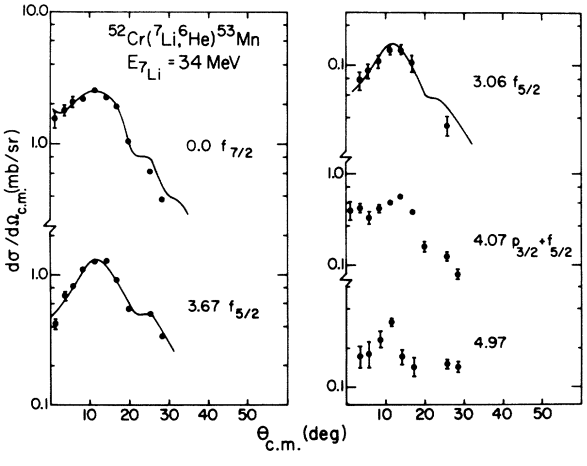

FIG. 7. Angular distributions for the ^{52}Cr(^{7}Li, ^{6}He)^{53}Mn reaction at 34 MeV. Levels shown are f-wave or are unresolved doublets of mixed final state orbital angular momentum. Solid lines are exact finite range DWBA calculations.

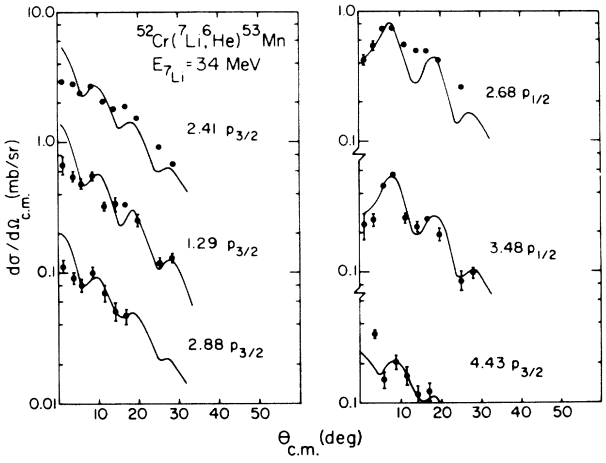

FIG. 8. Angular distributions for p-wave levels for the ^{52}Cr(^{7}Li, ^{6}He)^{53}Mn reaction. Solid lines are exact FRDWBA calculations.

reduced into angular distributions, this fact is highly suggestive that the entire cluster of levels should be assigned $l=4$. Lu, Zisman, and Harvey[20] have also observed $g_{9/2}$ strength at 6.4 MeV. Spectroscopic factors derived from comparing the experimental angular distributions with the calculations are given in Table I. These spectroscopic factors were deduced by using an extrapolation of the DWBA cross section.[21] The DWBA calculation was performed at several binding energies, -0.1, -0.5, and -1.0 MeV, and a linear extrapolation was made to the actual positive values "binding energy." For all of the binding energy calculations, the distorted wave information appropriate for the actual entrance and exit channel situation was used. Discussion of the validity of these spectroscopic factors and comparisons for the IAS levels to other experiments will be given later.

C. ^{52}Cr(^{7}Li,^{6}He)^{53}Mn reaction data

Angular distributions of the levels populated in the ^{52}Cr(^{7}Li, ^{6}He)^{53}Mn reaction at 34 MeV up to 5 MeV in excitation are shown in Figs. 7 and 8. The f-wave levels all show similar shapes in the angular distributions, with a peak at 12° (c.m.). These angular distributions are shown in Fig. 7 as well as those for the 4.07 and 4.96 MeV levels, which are unresolved doublets of mixed orbital angular momentum quantum numbers. The p-wave angular distributions are displayed in Fig. 8. Backward of 5° (c.m.), the angular distributions show similar shapes, which are dependent on the final state orbital angular momentum L with a peak at 8° (c.m.). However, several of the levels have angular distributions showing peaking forward of 5°, while other levels have angular distributions

which show no such peaking at the extreme forward angles. This is a J-dependent effect for the p-wave levels in the (^{7}Li, ^{6}He) reaction which was first studied by White *et al.*[22]

The J dependence for the final p states is expected on the basis of the well-known angular momentum selection rules. For the (^{7}Li, ^{6}He) reaction, since the transferred proton is in a bound $p_{3/2}$ orbit in the ^{7}Li projectile, the allowed transferred l values are $l=0,1,2$ for a final $p_{3/2}$ level, and $l=1,2$ for a final $p_{1/2}$ level. The "extra" $l=0$ component for the $p_{3/2}$ levels is expected to contribute at forward angles in the angular distributions.

The p-wave angular distributions which show forward angle peaking in our study can thus be assigned spins of $\frac{3}{2}$, while the other p-wave levels are assigned spins of $\frac{1}{2}$. The levels at 2.68 and 3.48 MeV are both determined to be $p_{1/2}$ levels from the lack of forward angle peaking in their angular distributions. Both these levels were initially considered to be $p_{3/2}$ levels by AB. The level at 2.68 MeV was revised to a $p_{1/2}$ assignment in a ^{52}Cr(α, t)^{53}Mn study at 22 MeV by Armstrong, Blair, and Thomas.[4] This reassignment of the spin was based principally on the fact that the 2.41 and 2.68 MeV levels angular distributions were out of phase. The level at 3.48 MeV was reassigned a spin of $\frac{1}{2}$ by Maripuu,[23] in a study of the ^{52}Cr(p, γ) ^{53}Mn reaction. This assignment was based on discrepancies in the branching ratios of the γ rays when a spin of $\frac{3}{2}$ was assumed.

The 4.43 MeV $l=1$ level is identified as being a $\frac{3}{2}$ level. This assignment is somewhat tentative as the forward angle peaking is only exhibited by the single data point at 3°. It was not possible to extract a reliable yield for this level at 1°. The $l=1$ component level of the 4.07 MeV doublet is likewise assigned as a $\frac{3}{2}$ level on the basis of the forward angle peaking which it exhibits. The level at 4.97 MeV exhibits no forward angle peaking and thus the p-state component is expected to be $p_{1/2}$.

The finite range DWBA code MERCURY[16] was used to calculate most of the angular distributions for comparison with the experimental results. For several of the angular distributions, the finite range DWBA code LOLA[24] was used. Comparison of calculations made on the same levels with these two codes result in identical shapes and magnitudes in agreement to a few percent. Since elastic scattering data were not taken and no optical model parameters exist for the ^{7}Li + ^{52}Cr or ^{6}He + ^{53}Mn systems, the optical parameters of White and Kemper[22] were used. The entrance channel parameters are from ^{7}Li scattering on ^{62}Ni at 34 MeV, and the exit channel parameters are from ^{6}Li scattering on ^{63}Cu at 30.1 MeV. These optical model parameters are listed in Table III. The calculations made with these parameters are shown in Figs. 7 and 8 with the data. The shapes of the angular distributions of the f-wave levels and of the $p_{1/2}$ levels are fairly well reproduced. The forward peaking for the $p_{3/2}$ levels is generally overestimated. The shape predicted by the calculation for the p states is generally more extreme than that present in the data, and a careful visual inspection indicates that the p-wave levels experimental angular distributions may be slightly out of phase with the calculations.

These problems with the calculations might be explained by the fact that the optical model parameters were not those derived from fitting elastic scattering data for ^{52}Cr + ^{7}Li or for ^{53}Mn + ^{6}He. However, it was felt that the optical model parameters used were from a case sufficiently close so that the use of the parameter set was justified. To make a simple test of this assumption, parameters for ^{40}Ca + ^{7}Li and ^{40}Ca + ^{6}Li at 20 MeV[25] were rather

TABLE III. Optical model parameters for the ^{52}Cr(^{7}Li, ^{6}He) ^{53}Mn reaction at 34 MeV. Parameters used as defined in Ref. 15.

Set	U (MeV)	r_R (fm)	a_R (fm)	W_S (MeV)	W_D (MeV)	r_I (fm)	a_I (fm)	r_C (fm)	λ
^{7}Li + ^{62}Ni [a]	49.72	1.78	0.58	8.52	···	1.78	1.01	1.78	
^{7}Li + ^{40}Ca [b] (Set A)	32.6	1.81	0.64	···	29.6	1.71	1.0	2.50	
^{6}Li + ^{63}Cu [a]	47.37	1.78	0.58	11.56	···	1.675	0.90	1.78	
^{6}Li + ^{40}Ca [b] (Set B)	31.0	1.72	0.81	···	53.2	1.69	0.80	2.50	
^{52}Cr + p	Var.	1.25	0.65					1.25	25
^{6}He + p	68.50	1.25	0.65					1.25	25

[a] Reference 21.
[b] Reference 24.

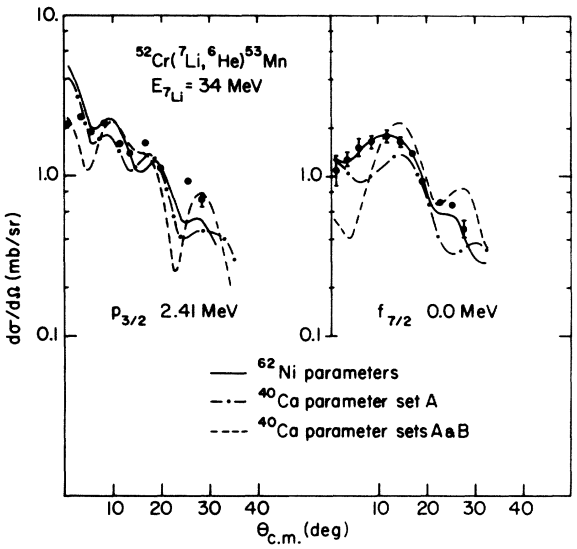

FIG. 9. Comparison of DWBA calculations made with various optical model sets for the ^{52}Cr(^{7}Li,^{6}He)^{53}Mn reaction at 34 MeV. The curve indicated as ^{62}Ni parameters used ^{7}Li + ^{62}Ni parameters in the entrance channel and ^{6}Li + ^{63}Cu parameters in the exit channel (parameters taken from Ref. 2). The curve marked Set A used Set A of Table III in both the entrance and exit channels. The curve marked Sets A&B used Set A in the entrance channel and Set B in the exit channel.

arbitrarily chosen as a set to make DWBA calculations for comparison with the calculations from the ^{62}Ni + ^{7}Li set. These optical model sets are listed in Table III. The same bound state parameters were used in all cases. Figure 9 shows a comparison of the calculations made with the various sets. In one calculation, the ^{7}Li + ^{40}Ca set was used in both the entrance and exit channels. In the other case, the ^{6}Li + ^{40}Ca parameter set was used for the exit channel distorted waves. The ^{62}Ni + ^{7}Li set generally gives a slightly better fit for the $p_{3/2}$ 2.41 MeV level and gives a much better result for the $f_{7/2}$ ground state.

It might be noted that the angular distribution for the $f_{7/2}$ ground state is somewhat different in shape from that of the $f_{5/2}$ 3.67 MeV level. This difference might be attributed to the difference in Q value causing dynamic changes in the angular distributions. It is true that this has a marked effect on the shape of the angular distribution. However, an additional factor in the difference in shape is a further J-dependent effect of the angular momentum selection rules. This effect has been previously reported and discussed for these data by Kemper *et al.*[26]

Spectroscopic factors from the (^{7}Li, ^{6}He) reaction are listed in Table I with the (^{3}He, d) spectroscopic factors. No renormalization has been made. Except for the ground state, where the C^2S differs by 25% possibly due to the large QDS band pass correction for the (^{3}He, d) data, all of the spectroscopic factors in the two reactions are in reasonable agreement.

IV. DISCUSSION

The spectroscopic factors determined in the (^{3}He, d) reaction are summed for each l_j and listed in Table IV. Levels of $l=1$ whose spins are not identified in the (^{7}Li, ^{6}He) reaction and were not previously known were included in the sum of the $p_{1/2}$ strength. All f-wave levels other than the ground state were considered to be $f_{5/2}$ levels for the purpose of summing the strength. The f-wave levels above 7 MeV were not included, as it is possible that these might be $T_>$ levels. Also shown in Table IV is the total strength expected from the shell model, using the simple formulas of Ref. 27.

Also shown in Table IV are the summed value of AB, corrected for the levels which were incorrectly identified. Too much strength is present in the $f_{5/2}$ orbit, and also in the $p_{1/2}$ orbit when it is realized that AB did not see the levels at 5.32 and 5.49 MeV. A second column shows the AB values adjusted for a normalization factor of 4.4 rather than the value of 3.7 which they used. These values are in good agreement with the values from this study, although they are systematically 15% higher. The summed values of OBDR are not included in this table, as corrections for the spin-orbit dependence in the bound state were not made. Shell model calculations have been made for ^{53}Mn,

TABLE IV. Summed strength from the ^{52}Cr(^{3}He,d) ^{53}Mn reaction and energy centroids for the strength for each orbit.

	$\sum C^2S$				$\langle E \rangle_{lj}$	
l_j	(^{3}He,d)	AB	AB×0.84	Theory	(^{3}He,d)	AB
$f_{7/2}$	0.23	0.47	0.39	0.50	0.0	0.0
$p_{3/2}$	0.45	0.66	0.56	0.80	2.71	2.60
$p_{1/2}$	0.55	0.79	0.66	0.80	4.04	3.94
$f_{5/2}$	0.57	0.86	0.72	0.80	4.14	4.01
$g_{9/2}$	(0.51)			0.80	(6.87)	

TABLE V. Spectroscopic factors for analog states seen in the $^{52}Cr(^3He,d)$ ^{53}Mn reaction and low lying levels seen in the ^{52}Cr (d,p) ^{53}Cr reaction.

l_j	$E(^3He,d)$	$S(^3He,d)$	$E(d,p)$	$S(d,p)$ [a]	$S(d,p)$ [b]	$S(d,p)$ [c]	ΔE
$p_{3/2}$	6.97	1.00	0.0	0.76	0.62	0.63	4.26
$p_{1/2}$	7.55	0.91	0.57	0.61	0.47	0.43	3.55
$f_{5/2}$	8.03	0.55	1.01	0.50	0.30	0.41	3.98

[a] Reference 28.
[b] Reference 29.
[c] Reference 30.

but these generally emphasize the electromagnetic quantities and the levels under 3 MeV, and their results are not very pertinent to this study. Lips and McEllistrem[28] have calculated the ground state spectroscopic factor to be 0.48 using simple configuration mixing. This value is, of course, much higher than our experimental value. However, it should be recalled that the choice of optical model sets used to analyze the $(^3He,d)$ reaction data could cause a difference of up to 50% in the absolute spectroscopic factors. Although the absolute spectroscopic factors from the $(^7Li,^6He)$ reaction agree very well with the $(^3He,d)$ values, this agreement could be fortuitous, as the optical model set used was not derived from appropriate elastic scattering data.

Energy centroid values for the l_j orbit strength are calculated from

$$\langle E\rangle_{lj}=\frac{\sum_i E_i C^2 S_i}{\sum_i C^2 S_i}$$

and are listed in Table IV. Centroid values from AB are also given. Although a centroid is given for the $g_{9/2}$ strength, this value is possibly too high as a large percentage of $g_{9/2}$ strength is thought to reside in the cluster of levels between 6.2 and 6.5 MeV which are not included.

In Table V, the spectroscopic factors for the three isobaric analog levels, multiplied by a factor of 5 to remove the C^2, are compared to spectroscopic factors for the three lowest levels in ^{53}Cr found in $^{52}Cr(d,p)^{53}Cr$ studies.[29-31] The values for the two p-wave isobaric analog are about 20% higher than those for the corresponding ^{53}Cr levels. Several factors should be taken into consideration, however. The extrapolation of the DWBA cross sections to determine the spectroscopic factors for the unbound isobaric analog levels may overestimate the spectroscopic factors. It is also likely that the experimental cross sections are somewhat overestimated because, in extracting the yields, a fixed, low background was used. The extracted cross sections could thus be systematically 7% to 20% too large. This problem is not shared by the isobaric analog state at 8.03 MeV as the background in this region was more certain. An important possible cause for the discrepancy is the isospin considerations for the $(^3He,d)$ reaction as pointed out by Cotanch and Robson[32]; there are two ways in which the conventional DWBA, as used in this study, can lead to anomalies in the spectroscopic factors due to the neglect of isospin. For the $(^3He,d)$ reaction, charge exchange coupling occurs for both the $T_>$ and $T_<$ levels; this results in destructive interference for $T_<$ states leading to smaller DWBA cross sections, and constructive interference for $T_>$ states, leading to larger theoretical cross sections than the conventional theory would predict. The second and stronger effect of including isospin involves the fact that there are many more available $T_<$ channels than $T_>$ channels to absorb flux. This is reflected by a larger absorption for the $T_<$ states than for the $T_>$ states. The inclusion of different absorptive potentials in the deuteron channel would be expected to affect the theoretical cross section in the same manner as the charge exchange coupling. While the effect is not expected to be dramatic for the $T_<$ states, the change predicted for the $T_>$ states by the DWBA cross sections would reduce the spectroscopic factors for each of the isobaric analog states. It is also pointed out by Cotanch and Robson that significant changes are only expected for the $(^3He,d)$ reaction where the final nucleus is populated through a definite $T_<$ or $T_>$ channel. For all other proton stripping reactions, such as (d,n) or $(^7Li,^6He)$, there is a unique total isospin coupling in the entrance channel through which the population of all levels in the residual nucleus, both $T_<$ and $T_>$, must proceed. In light of these uncertainties, it is felt that the spectroscopic factors for the isobaric analog states are in good agreement with those of their ^{53}Cr parent states.

Also shown in Table V are the values of $\Delta E = (E_> - \langle E_<\rangle)_{lj}$. A difference of 600 keV exists between the $p_{1/2}$ and $p_{3/2}$ values, and their average occurs at the value of ΔE of the $f_{5/2}$ orbit. This might suggest that some of the missing $p_{3/2}$ strength is still incorrectly identified as $p_{1/2}$. It should be noted that small changes in the identifi-

cation of $p_{1/2}$ strength as being actually $p_{3/2}$ will cause the $p_{3/2}$ $T_<$ centroid to shift dramatically upward, as the uncertain $p_{1/2}$ levels all lie at least 2 MeV higher than the $p_{3/2}$ centroid. Robson[33] has pointed out that the isospin energy splitting value ΔE can be a function of the shell orbit, and Philpott[34] has shown that this effect can cause shifts of 20% of the energy difference. This could account for the 600 keV spread in energy which is observed.

The authors would like to thank Gordon Morgan, Raymond Puigh, Gary Moore, Marty Hudson, Andy Obst, Mary Williams, Greg Norton, and Al Zeller for their help in the data taking. We appreciate the help of Mary E. Clark, Russell LeClaire, and Henry Kaufmann with the data analysis. For many informative discussions, we wish to thank Don Robson, William Courtney, Kirby Kemper, and Ron White. We would also like to express our appreciation to Mr. Bob Leonard for supplying us with targets and to the accelerator and electronics staffs at Florida State University for their invaluable assistance. Finally, we wish to thank Lowell Charlton and Ralph DeVries for their assistance with the FRDWBA codes MERCURY and LOLA.

---

*Research supported in part by the National Science Foundation Grants Nos. NSF-GP-25974, NSF-GU-2612, and NSF-GJ-367.

†Present address: Nuclear Structure Research Laboratory, University of Rochester, Rochester, New York 14627.

‡R. S. Mulliken Fellow in Physics.

[1]V. V. Okorokov, V. M. Serezhin, V. A. Smotryaev, D. L. Tolchenkov, I. S. Tronstin, V. N. Cheblukov, in Proceedings of the Eighteenth Annual Conference on Nuclear Spectroscopy and Structure of Atomic Nuclei, Riga, 1968 (unpublished), p. 118.

[2]J. J. Kent and R. C. Getz, Bull. Am. Phys. Soc. 19, 995 (1974).

[3]C. C. Lu, Ph.D. thesis, University of California, Berkeley, 1968, Report No. UCRL 18470, 1968 (unpublished).

[4]D. D. Armstrong, A. G. Blair, and H. C. Thomas, Phys. Rev. 155, 1254 (1967).

[5]D. D. Armstrong and A. G. Blair, Phys. Rev. 140, B1226 (1965).

[6]B. J. O'Brien, W. E. Dorenbusch, T. A. Belote, and J. Rapaport, Nucl. Phys. A104, 609 (1967).

[7]B. Cujec and I. M. Szöghy, Phys. Rev. 179, 1060 (1969).

[8]R. L. Auble and M. N. Rao, Nucl. Data B3, 137 (1970).

[9]I. Kohono, H. Kamitsubo, S. Nakajima, I. Yamane, M. Yoshie, and T. Mikaime, in Proceedings of the Symposium on Heavy Ion Transfer Reactions, Argonne, Illinois, 1973 [Argonne National Laboratory Informal Report No. PHY 1973B, 1973 (unpublished)], Vol. II, p. 573.

[10]K. Katori, M. Yoshie, I. Kohono, T. Mikumo, T. Motobayashi, S. Nakajima, and H. Kamitsubo, in *Proceedings of the International Conference on Reactions Between Complex Nuclei, Nashville, Tennessee, 1974,* edited by R. L. Robinson, F. K. McGowan, J. B. Ball, and J. H. Hamilton (North-Holland, Amsterdam/American Elsevier, New York, 1974), Vol. I, p. 58.

[11]E. Heinicke and H. Baumann, Nucl. Instrum. Methods 74, 229 (1969); E. Heinicke, K. Bethge and H. Baumann, *ibid.* 58, 125 (1968).

[12]G. R. Morgan, G. D. Gunn, M. B. Greenfield, N. R. Fletcher, J. D. Fox, D. L. McShan, and L. Wright, Nucl. Instrum. Methods 123, 439 (1975).

[13]P. D. Kunz, FORTRAN IV Program DWUCK, University of Colorado, Boulder, 1969 (unpublished).

[14]R. Stock, R. Bock, P. David, H. H. Duhm, and T. Tamara, Nucl. Phys. 104, 136 (1967).

[15]C. M. Perey and F. G. Perey, Phys. Rev. 132, 755 (1963)

[16]L. A. Charlton and D. Robson, Florida State University Technical Report No. 5, Tallahassee, 1969 (unpublished); L. A. Charlton, Phys. Rev. C 8, 146 (1973); 413 (1974).

[17]R. H. Bassel, Phys. Rev. 149, 791 (1966).

[18]T. K. Lim, Nucl. Phys. A129, 259 (1969).

[19]H. T. Fortune, T. J. Gray, W. Trost, and N. R. Fletcher, Phys. Rev. 179, 1033 (1969); H. T. Fortune, Ph.D. thesis, Florida State University, Tallahassee, 1974 (unpublished).

[20]C. C. Lu, M. S. Zisman, and B. G. Harvey, Phys. Lett. 27B, 217 (1968).

[21]M. B. Greenfield, C. R. Bingham, E. Newman, and M. J. Saltmarsh, Phys. Rev. C 6, 1756 (1972).

[22]R. L. White, K. W. Kemper, L. A. Charlton, and G. D. Gunn, Phys. Rev. Lett. 32, 892 (1974); R. L. White, Ph.D. thesis, Flordia State University, Tallahassee, 1974 (unpublished); R. L. White and K. W. Kemper, Phys. Rev. C 10, 1372 (1974).

[23]S. Maripuu, Nucl. Phys. A149, 593 (1970).

[24]R. M. DeVries, Phys. Rev. C 8, 951 (1973).

[25]K. Bethge, C. M. Fou, and R. W. Zurmühle, Nucl. Phys. A123, 521 (1969).

[26]K. W. Kemper, R. L. White, L. A. Charlton, G. D. Gunn, and G. E. Moore, Phys. Lett. 52B, 179 (1974).

[27]M. H. MacFarlane and J. B. French, Rev. Mod. Phys. 32, 567 (1960), as corrected by J. P. Schiffer in *Isospin in Nuclear Physics*, edited by D. H. Wilkinson (North-Holland, Amsterdam, 1969), p. 665.

[28]K. Lips and T. McEllistrem, Phys. Rev. C 1, 1009 (1970).

[29]D. C. Kocher and W. Haeberli, Nucl. Phys. A196, 225 (1972).

[30]G. Brown, A. Denning, and A. E. MacGregor, Nucl. Phys. A153, 145 (1970).

[31]R. Bock, H. H. Duhm, S. Martin, R. Rudel, and R. Stock, Nucl. Phys. 72, 273 (1965).

[32]S. Cotanch and D. Robson, Nucl. Phys. A209, 301 (1973); S. Cotanch, Ph. D. thesis, Florida State University, Tallahassee, 1973 (unpublished).

[33]D. Robson in *Nuclear Isospin*, edited by J. D. Anderson, S. D. Bloom, J. Cerny, and W. W. True (Academic, New York, 1969), p. 385.

[34]R. J. Philpott, Nucl. Phys. A179, 113 (1972).